Density Analysis of Intermolecular Orbital-Interaction Effects on the Second Hyperpolarizabilities of $\pi-\pi$ Stacking Dimers

Masayoshi Nakano,* Satoru Yamada, Masahiro Takahata, and Kizashi Yamaguchi

Department of Chemistry, Graduate School of Science, Osaka University, Toyonaka, Osaka 560-0043, Japan

Received: December 9, 2002; In Final Form: February 25, 2003

We investigate the intermolecular-interaction effects on the longitudinal second hyperpolarizabilities (γ) for $\pi-\pi$ stacking dimers of π-conjugated cation monomers, $C_5H_7^+$. Three types of geometrical configurations are examined to elucidate the relation between the longitudinal γ and the $\pi-\pi$ orbital interaction in the perpendicular direction to the monomer plane. The γ values are calculated by the finite-field (FF) approach using several ab initio molecular orbital (MO) and density functional (DF) methods. The spatial contributions of electrons to γ are analyzed using the plots of the second hyperpolarizability (γ) densities, which are described by the third-order derivatives of the charge densities with respect to the applied electric fields. It is found that the relative phase relation between interacting upper and lower π-orbitals is closely related to the intermolecular-interaction effects on γ of a dimer. Namely, in-phase (bonding-like) $\pi-\pi$ orbital interactions in the HOMO and HOMO−1 levels of a dimer tend to decrease the magnitude of γ density and then reduce the contribution to γ at the interacting sites. On the basis of this result, we discuss a novel guideline of controlling third-order nonlinear optical properties.

1. Introduction

For the last two decades, lots of theoretical and experimental studies on the third-order nonlinear optical (NLO) properties, which are described by the second hyperpolarizabilities (γ), for organic π-conjugated systems have been performed.[1−5] There have been many guidelines of designing molecules with large γ values and of controlling their features (sign and magnitudes).[5−9]

It is also well-known that these properties are affected by the intermolecular interaction, which causes the difference between the properties of isolated molecules and those of clusters or bulk materials. Actually, some guidelines of enhancing γ have been proposed on the basis of intermolecular charge-transfer (CT) effects, which lower the CT energy states.[10−14] In our previous papers,[10,12] we have investigated the features of intermolecular-interaction effects on γ in the stacking direction of several one-dimensional molecular aggregates, e.g., (A) mixed stacks, (B) neutral segregated stacks, and (C) mixed-valence segregated stacks (see Figure 1), which have been originally proposed as models of high-electric conducting molecular crystals.[15−17] It was found that system A, i.e., a Mott−Hubbard insulator, is a good candidate for systems with large γ in the stacking direction because system B has no CT due to large Coulomb interactions between neighboring monomers in the stacking direction and system C exhibits high-electric conductivity rather than high-electric polarization due to the significantly reduced Coulomb interaction for CT.[10,12] We have also proposed a unique multifunctional system using system C: the negative γ value, which is rare in general, is expected in the direction perpendicular to the stacking direction as well as high-electric conductivity.[13] In this case, the $\pi-\pi$ orbital interaction in the stacking direction is known to mainly contribute to the high-electric conductivity, whereas its effect on the γ in the perpendicular direction to the stacking direction has not been investigated.

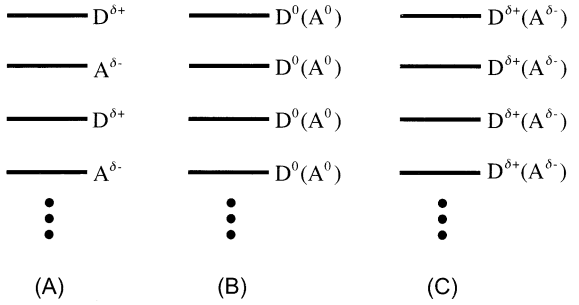

Figure 1. Three types of molecular aggregates: mixed (A), neutral segregated (B), and mixed-valence segregated (C) stacks. Each horizontal solid line indicates the monomer plane for D and/or A, which represent donor and acceptor molecules, respectively. The $\pi-\pi$ orbital interactions between molecular planes exist in the stacking direction. $\delta+$, $\delta-$, and 0 imply the slight-positively, slight-negatively, and noncharged states, respectively.

Recently, Ottonelli et al.[18] have investigated the intermolecular-interaction effects on the longitudinal α and γ of oligodiacetylene clusters in the INDO/S approximation.[19] They have found that in the $\pi-\pi$ stacking-type neutral and charged oligodiacetylene (composed of 15 units) clusters, some damping of γ per chain occurs with respect to that of an isolated chain. A similar situation is predicted to occur in the segregated stacks with $\pi-\pi$ interaction in the stacking direction. Namely, judging from their results, the $\pi-\pi$ stacking effects are predicted to reduce the magnitude of longitudinal γ, which is perpendicular to the stacking direction. To investigate the mechanism of such a feature, we consider three types of $\pi-\pi$ stacking dimer models (with the same intermolecular distance but different configurations) composed of $C_5H_7^+$, whose longitudinal component of γ is predicted to be negative in sign on the basis of our

* Corresponding author. E-mail: mnaka@cheng.es.osaka-u.ac.jp. Present address: Division of Chemical Engineering, Department of Materials Engineering Science, Graduate School of Engineering Science, Osaka University, Toyonaka, Osaka 560-8531, Japan.

10.1021/jp022558u CCC: $25.00
Published on Web 04/16/2003

classification rule of γ [9] and is considered to partially exist in the mixed-valence stacks (C).[13] The finite-field (FF) approach[20] using ab initio molecular orbital (MO) methods including several electron-correlation effects and density functional (DF) methods is applied to the calculation of longitudinal γ of these systems. The effects of $\pi-\pi$ orbital interactions are investigated by the second hyperpoalrizability (γ) density analysis,[21] which can elucidate the spatial contributions of electrons to γ. Namely, we focus on extracting the correlation rule among the feature of $\pi-\pi$ orbital overlaps of HOMOs of each monomer in the stacking direction and the longitudinal γ density distributions. On the basis of the structure−property relation obtained in this study, we propose a novel guideline of controlling third-order NLO properties using intermolecular orbital interaction.

2. Structure−Property Relation for Third-Order Nonlinear Optical Systems

Before investigating the intermolecular-interaction effects on the third-order nonlinear optical properties of dimers, we briefly explain our structure−property relation of γ for molecular systems.[5,9] This relation rule is derived on the basis of the fourth-order perturbation theory, which shows that static γ can be partitioned into the three types of virtual excitation processes (I, II, and III) as follows:[9]

$$\gamma^{\mathrm{I+II+III}} = \gamma^{\mathrm{I}} + \gamma^{\mathrm{II}} + \gamma^{\mathrm{III}} \tag{1}$$

where

$$\gamma^{\mathrm{I}} = \sum_{n=1} \frac{(\mu_{n0})^2(\mu_{nn})^2}{{E_{n0}}^3} \tag{2}$$

$$\gamma^{\mathrm{II}} = -\sum_{n=1} \frac{(\mu_{n0})^4}{{E_{n0}}^3} \tag{3}$$

and

$$\gamma^{\mathrm{III}} = \sum_{\substack{m,n=1 \\ (m\neq n)}} \frac{(\mu_{n0})^2(\mu_{mn})^2}{{E_{n0}}^2 E_{m0}} \tag{4}$$

Here, μ_{n0} is the transition moment between the ground and the nth excited states, μ_{mn} is the transition moment between the mth and the nth excited states, μ_{nn} is the difference of dipole moments between the ground and the nth excited states, and E_{n0} is the transition energy given by ($E_n - E_0$). These equations state that the contributions of types I and III are positive in sign, whereas the contribution of type II is negative. Typical conjugated molecular compounds with large positive γ are found to be classified to either case i $|\gamma^{\mathrm{I}}|, |\gamma^{\mathrm{III}}| \gg |\gamma^{\mathrm{II}}|$ ($\gamma > 0$) or case ii $|\gamma^{\mathrm{I}}| = 0$, $|\gamma^{\mathrm{II}}| < |\gamma^{\mathrm{III}}|$ ($\gamma > 0$). The compounds have large asymmetric charge distributions (which are responsible for large μ_{nn}) in case i and have centrosymmetric structures (which disappear type I) in case ii. Our classification rule predicts the existence of the third case, i.e., iii $|\gamma^{\mathrm{I}}| = 0$, $|\gamma^{\mathrm{II}}| > |\gamma^{\mathrm{III}}|$ ($\gamma < 0$), which is interesting because the systems with negative static γ is rare in general. Such systems tend to have symmetric structures ($\mu_{nn} = 0$) and to exhibit strong virtual excitation between the ground and the first excited states ($|\mu_{0n}| > |\mu_{nm}|$). This implies that the symmetric systems with large ground-state polarizability (α_0) tend to exhibit negative γ. We have proposed several symmetric conjugated molecular species, which are predicted to satisfy the case iii condition and have investigated their γ values by ab initio MO calculations including high-order electron-correlation effects.[13,22] It has been shown that those systems have a large contribution of resonances between polarized structures with mutually opposite directions.[22] This contribution leads to a reduction of the transition energy (E_{n0}) between the ground and the allowed first excited states. The contribution of stable resonance structures with large dipole moments also corresponds to an enhancement of the magnitude of the transition moment (μ_{n0}) between the ground and the allowed first excited states. In conclusion, a system with a large contribution of symmetric resonance structures with invertible polarization, which is referred to as SRIP, satisfies our criteria for the system to have a negative γ. For example, short-length symmetric charged linear chains, e.g., charged soliton-like π-conjugated oligomers, have large SRIP contributions and thus are expected to have negative longitudinal components of γ. This prediction has been confirmed by semiempirical and high-level ab initio MO calculations.[13,21,22] The symmetric small-size cation molecule, $C_5H_7^+$, used in this study has a large contribution of SRIP shown in Figure 2 and thus both the monomer and its $\pi-\pi$ stacking dimers are expected to exhibit negative γ values in the longitudinal direction. As shown in the next section, because SRIP systems generally tend to exhibit large electron-correlation effects on γ, several electron-correlation methods at the ab initio MO level as well as the DF methods are applied to the calculations of γ of these systems.

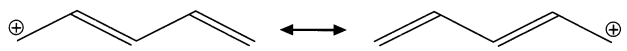

Figure 2. Symmetric resonance structure of invertible polarization (SRIP) of $C_5H_7^+$.

3. Methodology

3.1. Calculated Systems and Calculation Methods. Figure 3 shows the structures of monomer $C_5H_7^+$ (M) and three types of dimers (D-1), (D-2), and (D-3), in which the monomers lie in two $z-x$ planes (molecular planes) in a cofacial arrangement. These dimers have the same distance (van der Waals radius, 3.0 Å) between cofacial monomer planes and have different overlaps between upper and lower molecules in the stacking direction: (D-1) exhibits a complete overlap (**1-1′**, **2-2′**, **3-3′**, **4-4′**), whereas (D-2) and (D-3) show partial overlaps (**2-1′**, **3-2′**, **4-3′**, **5-4′** for (D-2) and **3-1′**, **4-2′**, **5-3′** for (D-3)). The geometry of the monomer is optimized under the C_{2v} symmetry using a hybrid DF, i.e., B3LYP,[23,24] method (using the 6-31G** basis set), which is known to well reproduce the geometry calculated by ab initio MO methods involving electron-correlation effects. The dimers are assumed to be built by simply assembling these monomers because we can neglect the geometry relaxation caused by the intermolecular interaction in this case. All calculations are performed by using the GAUSSIAN 98 program package.[25]

It is well-known that extended basis sets augmented by diffuse and polarization functions (p and d) are at least necessary for reproducing qualitative γ values for hydrocarbon compounds. It is also found that the basis set dependences are reduced for the γ in the longitudinal direction of larger-size systems though the basis set effects are not negligible for relatively small-size systems.[26] In the present study, we focus on qualitative or semiquantitative variations in the longitudinal γ for π-conjugated linear chain, so that the standard split-valence basis set 6-31G** is expected to be applied to such systems. However, the effects of such augmentation (diffuse p and d functions) on the weak

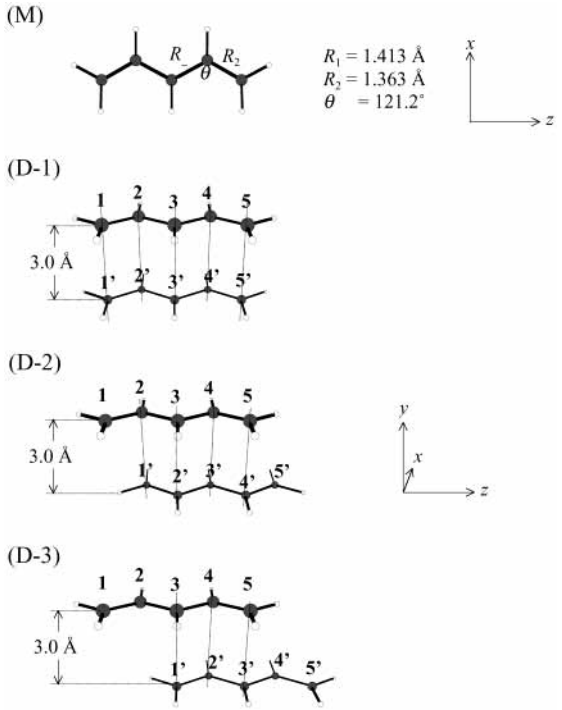

Figure 3. Structure of monomer ($C_5H_7^+$) (M) optimized by the B3LYP method with the 6-31G** basis set and three types of configurations of dimers, (D-1), (D-2), and (D-3). The monomers in dimers are put on the $z-x$ planes and the intermolecular distances between the cofacial planes are fixed to be 3.0 Å. The numbers **1**, **2**, **3**, **4**, and **5** (**1′**, **2′**, **3′**, **4′**, and **5′**) show the positions of carbon atom sites for an upper (lower) monomer.

TABLE 1: γ_{zzzz} Values Per Monomer (au) of the $C_5H_7^+$ Monomer and Its Dimer (D-1) (Figure 3) Calculated by the MP2 Level Using 6-31G and 6-31G**+pd**

	MP2/6-31G**	MP2/6-31G**+*pd*
monomer	−11270	−9689
dimer (D-1)	−5360	−4531

intermolecular interaction have not been investigated. We therefore examine the basis set dependency of longitudinal γ for monomer $C_5H_7^+$ and its dimer (D-1) (Figure 3) using extended basis sets augmented by the diffuse and polarization (p and d) functions (referred to as 6-31G**+pd ($\zeta_{p,d} = 0.0523$)) at the MP2 level (see section 4.1 for its validity concerning the inclusion of the electron-correlation effects on γ). The exponents of these functions are determined from the outermost two exponents of 6-31G** by the even-tempered method. The results (longitudinal γ/monomer) at the MP2 level are given in Table 1. Both the results of monomer and dimer using 6-31G**+pd are shown to be in good agreement with those by 6-31G** respectively though the magnitudes of γ by 6-31G**+pd slightly (14−15%) reduced as compared to those by 6-31G**. Therefore, the 6-31G** basis set is predicted to be sufficient for our semiquantitative study on the γ for the present systems.

In contrast, electron-correlation effects on γ for charged molecules are known to be remarkable,[5,13,21] so that we apply several ab initio MO methods: the Hartree−Fock (HF), the Møller−Plesset perturbation (MP2 and MP4), the quadratic configuration interaction (QCISD) and the coupled-cluster (CCSD and CCSD(T)) methods as well as the hybrid DF (BLYP,[24,27] B3LYP, and BHandHLYP[28]) methods, which can well reproduce the γ values of a small-size neutral π-conjugated molecule.[5,29] The HF, MP2, QCISD, and BHandHLYP methods are applied to the construction of γ density plots. It is noted that the QCISD method is known to be able to reproduce the total energy calculated by the CCSD method satisfactorily. Here the symbols S, D, and T denote the inclusion of the correlation effects caused by the single, double, and triple excitations, respectively. The CC and QCI methods can include these correlation effects to the infinite order.

We confine our attention to the longitudinal (z) components of γ (γ_{zzzz}) for these models. In the FF approach, the γ_{zzzz} value is calculated by the fourth-order numerical differentiation of the total energy E with respect to the applied field by

$$\gamma_{zzzz} = \{E(3F^z) - 12E(2F^z) + 39E(F^z) - 56E(0) + 39E(-F^z) - 12E(-2F^z) + E(-3F^z)\}/\{36(F^z)^4\} \quad (5)$$

Here, $E(F^z)$ indicates the total energy in the presence of the field F applied in the z direction. To avoid numerical errors, we use several minimum field strengths. After numerical differentiations using these fields, we adopt a numerically stable γ_{zzzz}, which is found to be obtained by using fields 0.001−0.002 au for these systems.

3.2. Seond Hyperpolarizability Density Analysis. We explain the static second hyperpolarizability (γ) density analysis in the FF approach. The charge density function $\rho(\mathbf{r},\mathbf{F})$ can be expanded in powers of the field F as[21,30]

$$\rho(\mathbf{r},\mathbf{F}) = \rho^{(0)}(\mathbf{r}) + \sum_j \rho_j^{(1)}(\mathbf{r})F^j + \frac{1}{2!}\sum_{jk}\rho_{jk}^{(2)}(\mathbf{r})F^jF^k + \frac{1}{3!}\sum_{jkl}\rho_{jkl}^{(3)}(\mathbf{r})F^jF^kF^l + \dots . \quad (6)$$

From this equation and the following expansion formula of the dipole moment in powers of the field:

$$\mu^i(\mathbf{F}) = -\int \mathbf{r}^i\rho(\mathbf{r},\mathbf{F})\,d\mathbf{r}^3 = \mu_0^i + \sum_j \alpha_{ij}F^j + \sum_{jk}\beta_{ijk}F^jF^k + \sum_{jkl}\gamma_{ijkl}F^jF^kF^l + \dots \quad (7)$$

the static γ can be expressed by[21]

$$\gamma_{ijkl} = -\frac{1}{3!}\int \mathbf{r}^i\rho_{jkl}^{(3)}(\mathbf{r})\,d\mathbf{r}^3 \quad (8)$$

where

$$\rho_{jkl}^{(3)}(\mathbf{r}) = \left.\frac{\partial^3\rho}{\partial F^j\partial F^k\partial F^l}\right|_{\mathbf{F}=0} \quad (9)$$

This third-order derivative of the electron density with respect to the applied electric fields is referred to as the γ density. In this study, we focus on the γ density ($\rho_{zzzz}^{(3)}(\mathbf{r})$), which is calculated at each spatial point in the discretized space by using the following third-order numerical differentiation formula.

$$\rho_{zzzz}^{(3)}(\mathbf{r}) = \{\rho(\mathbf{r},2F^z) - \rho(\mathbf{r},-2F^z) - 2(\rho(\mathbf{r},F^z) - \rho(\mathbf{r},-F^z))\}/2(F^z)^3 \quad (10)$$

where $\rho(\mathbf{r},F^z)$ represents the charge density at a spatial point r in the presence of the field F^z. The charge densities (at the HF, MP2, QCISD, and BHandHLYP levels) over a three-dimensional grid of points are evaluated by GAUSSIAN 98 program package.

To explain the analysis procedure by using the γ densities ($\rho_{zzzz}^{(3)}(\mathbf{r})$), let us consider a pair of localized $\rho_{zzz}^{(3)}(\mathbf{r})$ shown in Figure 4. The arrow from a positive (white circle) to a negative

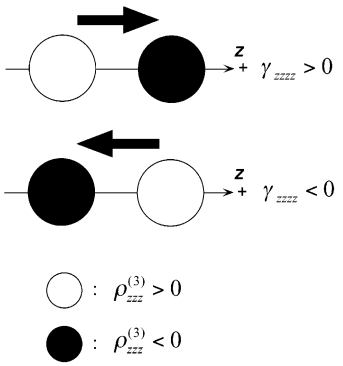

Figure 4. Schematic diagram of the second hyperpolarizability (γ) densities ($\rho^{(3)}_{zzz}(\mathbf{r})$). White and black circles represent positive and negative values of $\rho^{(3)}_{zzz}(\mathbf{r})$, respectively. The circle size represents the magnitude of $\rho^{(3)}_{zzz}(\mathbf{r})$, and the arrow shows the sign of $\rho^{(3)}_{zzz}(\mathbf{r})$ determined by the relative spatial configuration between the two $\rho^{(3)}_{zzz}(\mathbf{r})$ values.

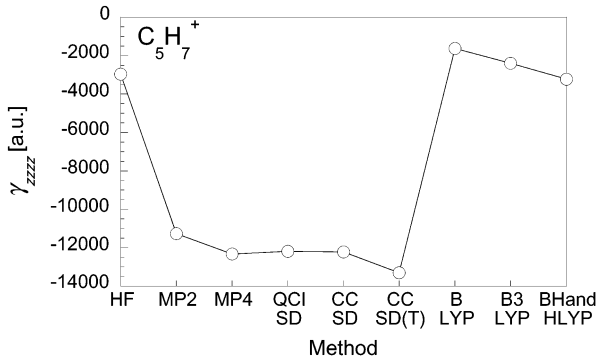

Figure 5. Variations of the γ_{zzzz} values of monomer (M) (Figure 2) for various ab initio MO (HF, MP2, MP4, QCISD, CCSD, and CCSD(T)) and DF (BLYP, B3LYP, and BHandHLYP) methods using the 6-31G** basis set.

(black circle) $\rho^{(3)}_{zzz}(\mathbf{r})$ shows the sign of the contribution determined by the relative spatial configuration between the two $\rho^{(3)}_{zzz}(\mathbf{r})$. Namely, the sign of the contribution becomes positive when the direction of the arrow coincides with the positive direction of the coordinate system. The contribution determined by the $\rho^{(3)}_{zzz}(\mathbf{r})$ of the two points is more significant, when their distance is larger. Of course, the magnitude of contribution to γ is in proportion to the magnitude of $\rho^{(3)}_{zzz}(\mathbf{r})$.

4. Results and Discussion

4.1. γ_{zzzz} Values and γ_{zzzz} Densities of a Monomer ($C_5H_7^+$). Figure 5 shows the electron-correlation effects on the longitudinal γ (γ_{zzzz}) of a monomer ($C_5H_7^+$). It is found that all the calculated γ_{zzzz} values are negative in sign, the feature of which is in agreement with our prediction based on the classification rule using the SRIP. The electron-correlation effect at the MP2 level is shown to significantly enhance the magnitude of γ_{zzzz} ($|\gamma_{zzzz}|$) at the HF level (-2965 au), which is about 4 times enhanced at the MP2 level (-11270 au). The electron-correlation effects at the MP4 (-12330 au), CCSD (-12220 au), QCISD (-12190 au), and CCSD(T) (-13300 au) levels are found to slightly increase the $|\gamma_{zzzz}|$ at the MP2 level. These results imply that a dominant electron-correlation effect on γ_{zzzz} comes from S and D contributions at the MP2 level for the present molecule. It is, however, shown that the DF methods cannot reproduce the sufficient magnitude of γ_{zzzz} at the MP2 level (-1628 au at the BLYP, -2396 au at the B3LYP, and -3229 au at the BHandHLYP). This suggests that the high-order polarizations of molecules with charged defects, which give significantly nonuniform charge distributions, are hard to describe by the present usual and hybrid DF methods.

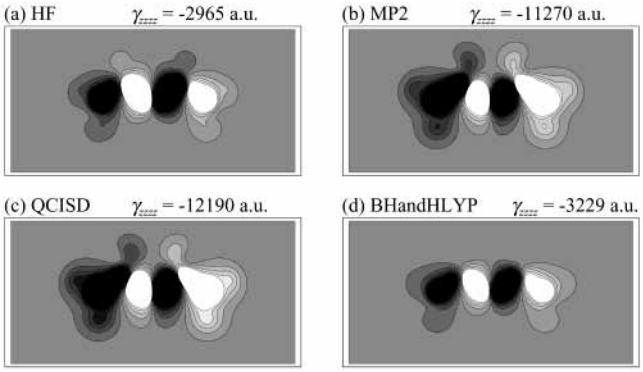

Figure 6. Contour plots of γ_{zzzz} densities ($\rho^{(3)}_{zzz}(\mathbf{r})$'s) on the plane located at 1 au above the molecular plane ($z-x$ plane in Figure 3) and γ_{zzz} values for various calculation methods. Contours are drawn from -100 to $+100$ au. Lighter areas represent the spatial regions with larger $\rho^{(3)}_{zzz}(\mathbf{r})$ values.

We next investigate the γ_{zzzz} density ($\rho^{(3)}_{zzz}(\mathbf{r})$) plots for the HF, MP2, QCISD, and BHandHLYP results (Figure 6) to clarify the difference in spatial contributions of π-electrons to γ_{zzzz} among these calculated results. The $\rho^{(3)}_{zzz}(\mathbf{r})$ values are drawn at the plane located at 1 au above the molecular plane ($z-x$ plane) to examine the contribution of π-electrons. All the methods provide the same qualitative feature of contribution, e.g., phase of $\rho^{(3)}_{zzz}(\mathbf{r})$, in which both end regions (**1**-**2** and **4**-**5**) give large negative contributions in contrast to the internal small regions (**2**-**3**-**4**) with small positive contributions. This feature leads to the total negative γ_{zzzz}. The feature of $\rho^{(3)}_{zzz}(\mathbf{r})$ at the MP2 and QCISD levels are shown to be in good agreement with each other and their both-end contributions are more extended than those at the HF and BHandHLYP levels, which are also similar to each other. This difference in the features of $\rho^{(3)}_{zzz}(\mathbf{r})$ between the HF (BHandHLYP) and MP2 (QCISD) methods supports the difference between their γ_{zzzz} values shown in Figure 5. As a result, the semiquantitative features of γ_{zzzz} and $\rho^{(3)}_{zzz}(\mathbf{r})$ for $C_5H_7^+$ are found to be well described at the MP2 level. We therefore use the MP2 method to calculate the γ_{zzzz} values and $\rho^{(3)}_{zzz}(\mathbf{r})$ distributions for dimers because the intermolecular interaction with van der Waals radius is relatively weak. It is noted that this does not imply the applicability of MP2 to the γ for any charged molecules because higher-order electron-correlation methods beyond the MP2 level are shown to be necessary for obtaining converged γ values for some charged radical systems.[22]

4.2. γ_{zzzz} Values and γ_{zzzz} Densities of Dimers. It is found that the γ_{zzzz} values at the MP2 level of dimers, (D-1), (D-2), and (D-3), are $-10\,720$, $-13\,590$, and $-16\,510$ au, respectively. As compared with the γ_{zzzz} values (-11270 (monomer) x 2 = -22540 au) of a dimer without intermolecular interaction, the intermolecular interaction is predicted to significantly reduce the magnitude of γ_{zzzz} value per monomer. This feature is similar to the results of the longitudinal γ of oligodiacetylene clusters obtained by Ottonelli et al.[18] Further, the magnitude of reduction of γ_{zzzz} per monomer is shown to be more significant when the number of overlapped sites between the upper and lower monomers increases.

To better elucidate the structure−property relation of such a change in γ_{zzzz} value, the γ_{zzzz} density ($\rho^{(3)}_{zzz}(\mathbf{r})$) plots of these systems are examined. Figure 7 shows the isosurfaces of

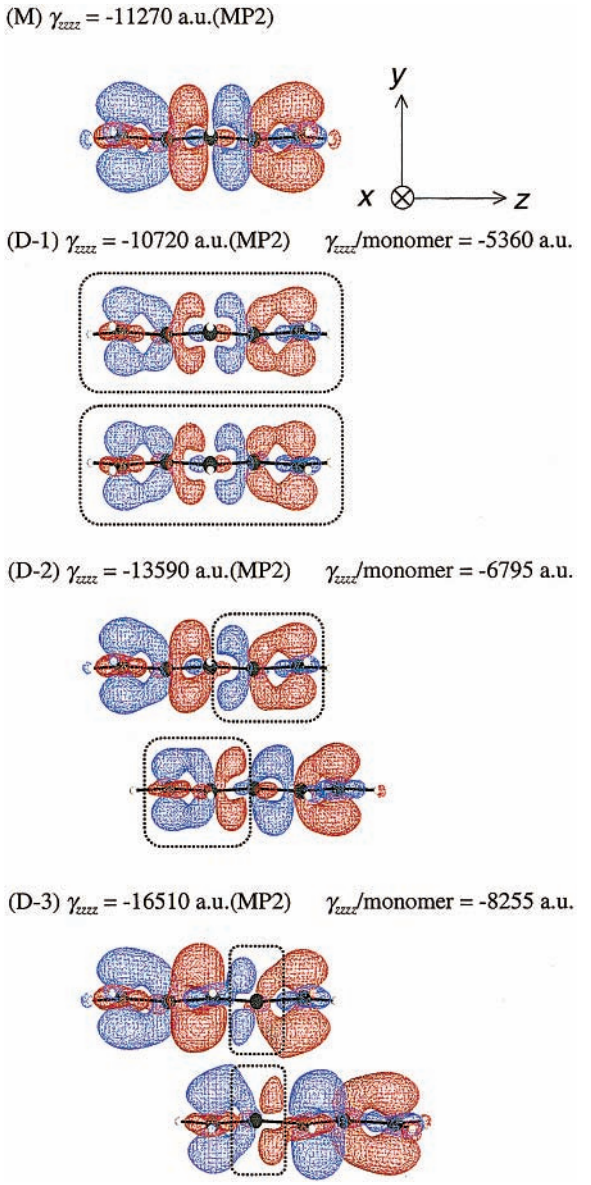

Figure 7. Isosufaces (red mesh for 100 au and blue mesh for −100 au) of γ_{zzz} densities ($\rho^{(3)}_{zzz}(\mathbf{r})$'s) of monomer (M) and dimers (D-1)−(D-3). The regions circled by dotted lines indicate the significant reduction regions of $|\rho^{(3)}_{zzz}(\mathbf{r})|$ as compared to those of monomer (M).

$\rho^{(3)}_{zzz}(\mathbf{r})$ for (D-1), (D-2), and (D-3) as well as those for the monomer (M). The isosurfaces of $\rho^{(3)}_{zzz}(\mathbf{r})$ with +100 and −100 au are drawn in red and blue three-dimensional meshes, respectively. For the completely overlapped dimer (D-1), significant reductions of magnitudes of $\rho^{(3)}_{zzz}(\mathbf{r})$ for upper and lower monomers are observed on all sites, whereas for the partially overlapped dimers (D-2) and (D-3), partial reductions of $\rho^{(3)}_{zzz}(\mathbf{r})$ are observed. Although the number of reduction sites of $\rho^{(3)}_{zzz}(\mathbf{r})$ for these dimers corresponds to the magnitudes of reduction of $|\gamma_{zzzz}|$, it is noted that such reduction regions do not necessary coincide with the overlapped sites. For example, for (D-2), **2**-**1**′, **3**-**2**′, **4**-**3**′, and **5**-**4**′ are overlapped, whereas the reductions of $\rho^{(3)}_{zzz}(\mathbf{r})$ are observed at sites **4**-**5** for an upper monomer and sites **1**′-**2**′ for a lower monomer. In particular, for (D-3), the primary reductions of $\rho^{(3)}_{zzz}(\mathbf{r})$ appear only at sites **4** and **2**′ though sites **3**-**1**′, **4**-**2**′, and **5**-**3**′ are overlapped.

To interpret the above reduction feature of $\rho^{(3)}_{zzz}(\mathbf{r})$, we make a hypothesis based on the virtual excitation process (explained in section 2) and the π-orbital overlaps in the stacking direction.

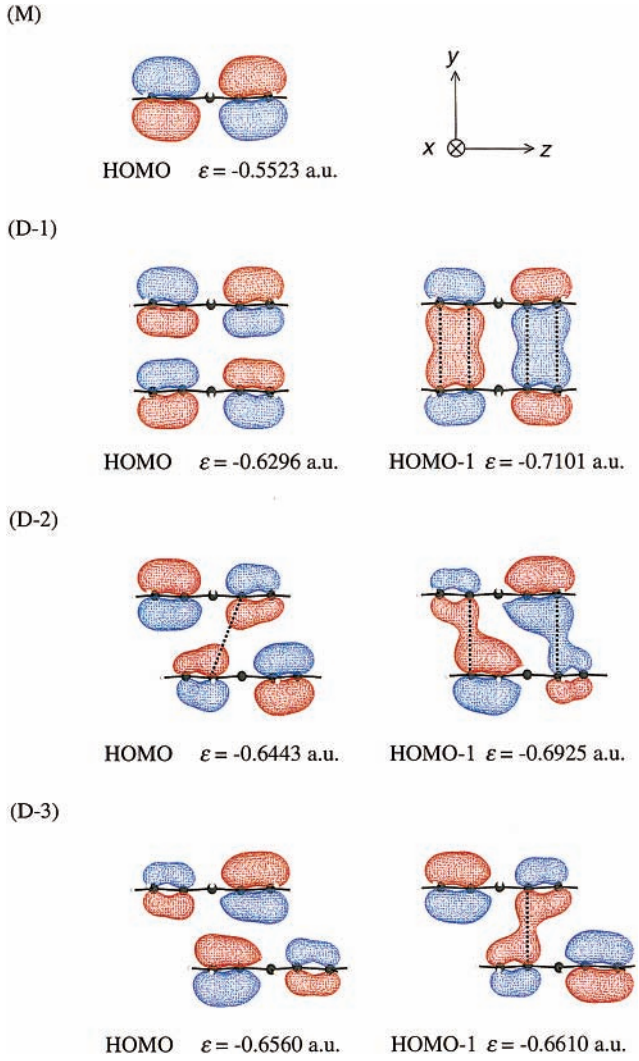

Figure 8. Isosurfaces (red mesh for 0.04 au and blue mesh for −0.04 au) of the HOMO and HOMO−1 orbitals for dimers (D-1)−(D-3) as well as those of the HOMO orbital for monomer (M). The energies of the HOMO and HOMO−1 levels are also shown. The dotted lines show the bonding-like (in-phase) $\pi-\pi$ orbital interactions between upper and lower monomers.

As shown in section 2, all the virtual excitation processes contributing to γ start from and return back to the ground state. In the present case, such virtual excitations are predicted to be primarily described by the longitudinal virtual transfer of π-electrons in the HOMO of a dimer. In addition, some in-phase (bonding-like) overlaps between π-orbitals of upper and lower monomers are expected at the overlapped sites in the stacking direction. We speculate that the longitudinal virtual transfer of π-electrons is reduced by somewhat locking the π-electrons at sites with bonding-like overlaps between upper and lower π-orbitals. Further, the position of orbital−orbital interaction will be important for systems with large π-conjugation because the segmentation of a long π-conjugation pathway into smaller ones by such orbital interactions is predicted to cause a reduction of the magnitude of γ.

4.3. Orbital-Interaction Effects on the Longitudinal γ of Dimers. To confirm our speculation, we investigate the HOMO and HOMO−1 of these dimers as well as the HOMO of a monomer at the HF level (see Figure 8). Although the magnitude of γ_{zzzz} value of a monomer at the HF level is smaller than that at the MP2 level (see Figure 5), the qualitative features concerning orbital relative phases and relative stability of the

HOMO and HOMO−1 of dimers are sufficient for our discussion. As easily expected from the two kinds of combination of HOMOs of monomers (Figure 8 (M)), the dimers have the two near-degenerate HOMO and HOMO−1, which become completely degenerate in the case of nonintermolecular interaction. The bonding- and antibonding-like interactions between the upper and lower monomers slightly split the degenerate HOMOs of noninteracting dimers, and the combination of HOMOs of monomers in the HOMO and HOMO−1 of dimers can be predicted by considering neighboring bonding- and antibonding-like interactions between monomers. As is well-known, the contribution of HOMO(π)−LUMO(π^*) transition energy is a good approximation to the first excitation energy involved in the virtual excitation processes of γ. The enhancement of this transition energy contributes to the reduction of the magnitude of each type of contribution to γ (see eqs 2−4). In the present case, therefore, the stabilization of the HOMO of a monomer due to the bonding-like interaction between upper and lower monomers is expected to increase the corresponding $\pi-\pi^*$ energy gap and then to reduce the contribution of π-electrons, which participate in the bonding-like interaction, to longitudinal γ. Namely, the in-phase (bonding-like) overlap of π-orbitals between upper and lower monomers tends to reduce the feasibility of longitudinal virtual transfer of π-electrons contributing to the bonding-like interaction. Such bonding-like interaction is also expected to reduce the magnitude of transition moment in the longitudinal direction of each monomer because the spatial distribution of the HOMO of monomer is somewhat pinned on the bonding-like interaction sites. As a result, we can generally say that the bonding-like interaction in the stacking direction at a site tends to lock the π-electrons at the interacting site. Further, if such bonding-like interactions slightly interrupted a π-conjugation pathway, the virtual transfer through this pathway would be somewhat suppressed. As shown in Figure 8, HOMO and HOMO−1 energies for these dimers are lower than the HOMO energy of a monomer, indicating that there exists some bonding-like interactions in the HOMO and HOMO−1 of these dimers. We next elucidate the details of relations among bonding-like interactions in the HOMO and HOMO−1 and the locking of π-electrons contributing to the longitudinal virtual transfer in each dimer model.

For (D-1), the primary bonding (in-phase) and antibonding (out-of-phase) interactions are observed between all overlapped sites of the HOMO−1 and HOMO, respectively, because of the completely overlapped structure between upper and lower monomers. Only slight lockings of π-electrons are expected in the HOMO of (D-1) due to their primary antibonding-like interaction at each site between upper and lower monomers, whereas the significant lockings of π-electrons in the HOMO−1 are predicted to contribute to the reduction of longitudinal γ. This interaction feature in the HOMO−1 supports the reduction of $\rho_{zzz}^{(3)}(\mathbf{r})$ at all sites for (D-1). In the HOMO of (D-2), somewhat bonding-like interactions are expected between neighboring sites **4** and **2′**, whereas others are mainly antibonding-like interactions. It is also noted that **3**-**2′** and **4**-**3′** interactions vanish due to the disappearance of orbital distribution at sites **3** and **3′**. Therefore, orbital interactions in the HOMO of (D-2) cause the locking of π-electrons at sites **4** and **2′** but no locking at sites **1**-**2** and **4′**-**5′**. The near-degenerate HOMO−1 shows significant bonding-like interactions between sites **2**(**5**) and **1′**(**4′**). Judging from the orbital interactions in the HOMO and HOMO−1 of (D-2), the primary lockings of π-electrons are expected at sites **4**-**5** and **1′**-**2′** because the π-electrons at **1**-**2** and **4′**-**5′**, which are partially locked in the HOMO−1, are not locked in the HOMO. For (D-3), the HOMO is not shown to contribute to the significant locking of π-electrons because the neighboring π-orbitals are mutually antibonding. In contrast, the bonding-like interaction between sites **4** and **2′** in the HOMO−1 of (D-3) is predicted to lock the π-electrons at sites **4** and **2′**. It is noted that the π-electrons at sites **3**, **1′**, **5**, and **3′** of (D-3) are not locked because of the disappearance of π-orbital distributions at sites **3** and **3′** in the HOMO and HOMO−1. This feature leads to the reduction of $\rho_{zzz}^{(3)}(\mathbf{r})$ only at sites **4** and **2′** of (D-3).

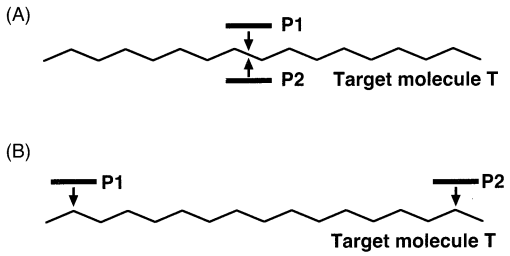

Figure 9. Model systems (A and B) of controlling longitudinal γ of a target molecule T by intermolecular orbital interaction. P1 and P2 indicate perturbation molecules with bonding-like interaction and the arrows indicate the positions of such interactions.

In conclusion, the reduction region of $\rho_{zzz}^{(3)}(\mathbf{r})$ for a dimer can be predicted by using the distribution $\rho_{zzz}^{(3)}(\mathbf{r})$ of a monomer and the bonding-like π-orbital interactions in the HOMO and HOMO−1 of a dimer, which is easily estimated by considering the combination of HOMOs of monomers. Such a structure−property relation using the effects of orbital interactions on γ can be extended to more general systems, not limited to dimers composed of the same monomers, and will be useful for a control of third-order NLO properties. Let us consider a model system composed of a large one-dimensional π-conjugated molecule (target system) T and small-size molecules (chemical perturabtion) P1 and P2, which are used for locking the π-orbitals of the HOMO of T (see Figure 9). It is assumed that the longitudinal γ of T is much larger than that of P1(P2), so that the γ of total system could be well approximated to be that of T if the intermolecular interaction between T and P1 (P2) were negligible. In this model, the bonding-like interaction between P1(P2) and T may slightly destabilize the HOMO of T in contrast to the $C_5H_7^+$ dimer case studied because the overlapped sites are restricted to small regions and such interactions tend to attenuate the longitudinal bonding interaction in T. However, the longitudinal transition moments of T, which represent the feasibility of virtual charge transfer along the linear chain direction, are predicted to be reduced corresponding to the degree of interruption of π-conjugation caused by the bonding-like interaction between P1(P2) and T. Such interception effects will be more remarkable in γ than in α because the virtual charge transfer over a more extended region is essential for describing γ. We consider the longitudinal total γ for two cases: (A) both P1 and P2 are located in the middle of T, whereas (B) P1 and P2 are located respectively at both-end regions of T. We here assume a bonding-like interaction between P1(P2) and T. As predicted from the present results, these bonding-like interactions tend to suppress the longitudinal virtual charge transfer of π-electrons of T. In case (A), the longitudinal γ for T is predicted to be reduced because the π-conjugation is partially interrupted at the middle point of the chain, whereas in case (B) the longitudinal γ will not be so reduced or has a possibility of being enhanced instead. This can be understood as follows. In case (B), the π-conjugation length is only slightly decreased due to the both-end locking, and somewhat virtual

charge transfer is also expected between P1 and P2 via the π-conjugation bridge of T because such weak bonding-like interaction in the stacking direction is not predicted to completely lock the electrons at the interacting sites. It is noted that the P1 and P2 almost overlap with each other in the same region in case (B), whereas those are located with large distance in the end region of the chain. Namely, the relative positions of perturbation molecules, which have bonding orbital interactions with the target molecule, are predicted to be important for controlling the γ value of the total system. It is further speculated that we may even control the sign of total γ by getting perturbation molecules to approach and to suppress the virtual charge transfer of electrons in the regions with positive or negative contributions (which can be specified by the γ density analysis) of target molecule.

It is worthwhile that we here speculate the effects of relative charges for monomers on the γ for dimers. The present study suggests for dimers composed of cation monomers that the bonding-like orbital interaction between upper and lower monomers tend to attenuate the virtual charge transfer in the longitudinal direction and then decrease the longitudinal γ of the monomer. What would happen in the case of dimer composed of neutral monomers? On the basis of the present results that orbital overlap interaction is the primary reason of the decrease in the longitudinal γ, similar tendency is expected to be observed because such bonding-like interactions also exist in dimer composed of neutral monomers. As an example, we calculate the longitudinal γ for the dimer (singlet state) ((D-1) type shown in Figure 3) composed of neutral $C_5H_7^{\bullet}$ (doublet state). Because at such a large distance (3.0 Å) the singlet UHF based method is expected to provide a good approximate solution for the dimer, we calculate γ for the monomer and dimer at the UHF/6-31G** level (in this case, the UCCSD(T) results (the most accurate results) are found to be well reproduced at the UHF level.). It is found that the γ (monomer) is 9493 au, whereas the γ/monomer for the dimer is 5278 au. The positive values of γ for these systems can be understood by considering the small contribution of SRIP in $C_5H_7^{\bullet}$. As expected, a remarkable reduction of longitudinal γ is observed for such a neutral dimer, similarly to the present results for cation systems. In the case of longitudinal γ for dimer composed of a positive and negative ion pair, more reduction of γ may occur because the π-electrons are more significantly locked around the interacting sites (which causes the further reduction of longitudinal transition moments) due to the electrostatic attractive force in addition to the orbital overlap effects.

5. Concluding Remarks

In this study, we investigated the longitudinal γ values of three types of dimers (with different overlap configurations) constructed from a symmetric charged molecule, $C_5H_7^{+}$, which is predicted to exhibit a negative γ value on the basis of our classification of γ. From the analysis of γ density distributions and the HOMO and HOMO-1 orbitals of dimers, we found that the $\pi-\pi$ bonding-like (in-phase) orbital interaction in the stacking direction tends to lock the π-electrons, which dominantly contributes to the longitudinal γ at the interacting sites. Actually, the magnitudes of γ densities (with negative contributions) at sites with bonding-like interactions are reduced, and thus the magnitude of total γ for a noninteracting dimer is shown to be reduced. Our structure$-$property relation of γ based on the orbital interaction between monomers is shown to be able to well interpret the differences in γ values and γ density distributions among these dimer models. The orbital-interaction effects on γ obtained in this study are useful for the interpretation of the intermolecular-interaction effects on γ values of cluster and bulk systems. On the other hand, on the basis of such orbital-interaction effects on γ, we speculated a novel control scheme of γ values of molecular-based nanostructured systems by intermolecular orbital interactions between the target and other small-size molecules. The validity of such a control scheme based on the orbital interaction between HOMOs will be investigated using several π-conjugated model systems, including different-charged monomer pairs, at the next stage.

Acknowledgment. This work was supported by Grant-in-Aid for Scientific Research (No. 14340184) from the Japan Society for the Promotion of Science (JSPS) and a Grant from the Ogasawara Foundation for the Promotion and Science & Engineering.

References and Notes

(1) Williams, D. J., Ed. *Nonlinear Optical Properties of Organic and Polymeric Materials*; ACS Symposium Series 233; American Chemical Society: Washington, DC, 1984.

(2) Prasad, N. P.; Williams, D. J. *Introduction to Nonlinear Optical Effects in Molecules and Polymers*; Wiley: New York, 1991.

(3) Nalwa, H. S., Ed. *Nonlinear Optical Materials*; Handbook of Advanced Electronic and Photonic Materials and Devices, Vol. 9; Academic Press: New York, 2001.

(4) (a) Kanis, D. R.; Ratner, M. A.; Marks, T. J. *Chem. Rev.* **1994**, *94*, 195. (b) Brédas, J. L.; Adant, C.; Tackx, P.; Persoons, A. *Chem. Rev.* **1994**, *94*, 243.

(5) (a) Nakano, M.; Yamaguchi, K. Analysis of nonlinear optical processes for molecular systems. *Trends in Chemical Physics*; Research trends: Trivandrum, India, 1997; Vol. 5, pp 87$-$237. (b) Nakano, M.; Yamaguchi, K. Polarizabilities and hyperpolarizabilities of dendritic systems. *Advances in multi-photon processes and spectroscopy*; World Scientific, Vol. 15, p 1.

(6) Kajzar, F.; Messier, J. In *Conjugated Polymers*, Brédas; J. L., Silbey, R., Eds.; Kluwer: Dordrecht, The Netherlands, 1991; p 509.

(7) Heflin, J. R.; Wong, K. Y.; Zamani-Khamiri, O.; Garito, A. F. *Phys. Rev. B* **1988**, *38*, 1573.

(8) Pierce, B. M. *J. Chem. Phys.* **1989**, *91*, 791.

(9) (a) Nakano, M.; Okumura, M.; Yamaguchi, K.; Fueno, T. *Mol. Cryst. Liq. Cryst.* 1990, *182 A*, 1. (b) Nakano, M.; Yamaguchi, K. *Chem. Phys. Lett.* **1993**, *206*, 285.

(10) (a) Nakano, M.; Yamaguchi, K.; Fueno, T. *Kobunshi Ronbunshu* **1990**, *47*, 779. (b) Nakano, M.; Yamaguchi, K.; Fueno, T. In *Computer Aided Innovation of New Materials*; Doyama, M., Suzuki, T., Kihata, J., Yamamoto, R., Eds.; Elsevier: Amsterdam, 1991; p 259.

(11) Gotoh, T.; Kondoh, T.; Egawa, K. *J. Opt. Soc. Am. B* **1990**, *6*, 703.

(12) Nakano, M.; Yamaguchi, K.; Fueno, T. *Nonlinear Opt.* **1994**, *6*, 289.

(13) (a) Nakano, M.; Yamada, S.; Yamaguchi, K. *Chem. Phys. Lett.* **1999**, *311*, 221. (b) Nakano, M.; Yamada, S.; Yamaguchi, K. *J. Phys. Chem. A* **1999**, *103*, 3103.

(14) Kisida, H.; Matsuzaki, H.; Okamoto, H.; Manabe, T.; Yamashita, M.; Taguchi, Y.; Tokura, Y. *Nature* **2000**, *405*, 929.

(15) Gutmann, F.; Lyons, J. E. *Organic Semiconductors*; Wiley: New York, 1967.

(16) Soos, Z. G. *Annu. Rev. Phys. Chem.* **1974**, *25*, 121.

(17) Torrance, J. B. *Acc. Chem. Res.* **1979**, *12*, 79.

(18) (a) Ottonelli, M.; Musso, G. F.; Comoretto, D.; Dellepiane, G. *Phys. Chem. Cem. Phys.* **2002**, *4*, 2754. (b) Ottonelli, M.; Musso, G. F.; Comoretto, D.; Dellepiane, G. *Synth. Met.*, in press.

(19) Ridley, J.; Zerner, M. C. *Theor. Chim. Acta* **1973**, *32*, 111; **1976**, *42*, 223; **1979**, *53*, 21.

(20) (a) Cohen, H. D.; Roothaan, C. C. J. *J. Chem. Phys.* 1965, *S34*, 43. (b) Karna, S. P.; Prasad, S. P.; Dupuis, M. *J. Chem. Phys.* **1991**, *94*, 1171.

(21) (a) Nakano, M.; Yamaguchi, K.; Fueno, T. *Chem. Phys. Lett.* **1991**, *185*, 550. (b) Nakano, M.; Shigemoto, I.; Yamada, S.; Yamaguchi, K. *J. Chem. Phys.* **1995**, *103*, 4175. (c) Nakano, M.; Yamada, S.; Shigemoto, I.; Yamaguchi, K. *Chem. Phys. Lett.* **1996**, *250*, 247. (d) Nakano, M.; Fujita, H.; Takahata, M.; Yamaguchi, K. *Chem. Phys. Lett.* **2002**, *356*, 462.

(22) (a) Nakano, M.; Kiribayashi, S.; Yamada, S.; Shigemoto, I.; Yamaguchi, K. *Chem. Phys. Lett.* **1996**, *262*, 66. (b) Nakano, M.; Yamada,

S.; Yamaguchi, K. *Int. J. Quantum Chem.* **1998**, *70*, 269. (c) Nakano, M.; Yamada, S.; Yamaguchi, K. *Bull. Chem. Soc. Jpn.* **1998**, *71*, 845. (d) Yamada, S.; Nakano, M.; Yamaguchi, K. *J. Phys. Chem. A* **1999**, *103*, 7105.

(23) Becke, A. D. *J. Chem. Phys.* **1993**, *98*, 5648.

(24) Lee, C.; Yang, W.; Parr, R. G. *Phys. Rev. B* **1988**, *37*, 785.

(25) Frisch, M. J.; Trucks, G. W.; Schlegel, H. B.; Scuseria, G. E.; Robb, M. A.; Cheeseman, J. R.; Zakrzewski, V. G.; Montgomery, J. A.; Stratmann, R. E.; Burant, J. C.; Dapprich, S.; Millam, J. M.; Daniels, A. D.; Kudin, K. N.; Strain, M. C.; Farkas, O.; Tomasi, J.; Barone, V.; Cossi, M.; Cammi, R.; Mennucci, B.; Pomelli, C.; Adamo, C.; Clifford, S.; Ochterski, J.; Petersson, G. A.;. Ayala, P. Y.; Cui, Q.; Morokuma, K.; Malick, D. K.; Rabuck, A. D.; Raghavachari, K.; Foresman, J. B.; Cioslowski, J.; Ortiz, J. V.; Stefanov, B. B.; Liu, G.; Liashenko, A.; Piskorz, P.; Komaromi, I.; Gomperts, R.; Martin, R. L.; Fox, D. J.; Keith, T.; Al-Laham, M. A.; Peng, C. Y.; Nanayakkara, A.; Gonzalez, C.; Challacombe, M.; Gill, P. M. W.; Johnson, B. G.; Chen, W.; Wong, M. W.; Andres, J. L.; Head-Gordon, M.; Replogle, E. S.; Pople, J. A. *Gaussian 98*, revision A.1; Gaussian, Inc.: Pittsburgh, PA, 1998.

(26) (a) Hurst, G. J. B.; Dupuis, M.; Clementi, E. *J. Chem. Phys.* **1988**, *89*, 385. (b) Nakano, M.; Fujita, H.; Takahata, M.; Yamaguchi, K. *J. Am. Chem. Soc.* **2002**, *124*, 9648. (c) Yamada, S.; Nakano, M.; Shigemoto, I.; Yamaguchi, K. *Chem. Phys. Lett.* **1996**, *254*, 158.

(27) Becke, A. D. *Phys. Rev. A* **1988**, *38*, 3098.

(28) Becke, A. D. *J. Chem. Phys.* **1993**, *98*, 1372.

(29) (a) Matsuzawa, N.; Dixon, D. A. *J. Phys. Chem.* **1994**, *98*, 2545. (b) Calaminici, P.; Jug, K.; Köester, A. M. *J. Chem. Phys.* **1998**, *109*, 7756. (c) Yamada, S.; Nakano, M.; Shigemoto, I.; Yamaguchi, K. *Chem. Phys. Lett.* **1996**, *254*, 158.

(30) Chopra, P.; Carlacci, L.; King, H.; Prasad, P. N. *J. Phys. Chem.* **1989**, *93*, 7120.